Global Change Biology (2004) **10,** 1180–1196, doi: 10.1111/j.1365-2486.2004.00798.x

Short- and long-term greenhouse gas and radiative forcing impacts of changing water management in Asian rice paddies

STEVE FROLKING*, CHANGSHENG LI*, ROB BRASWELL* and JAN FUGLESTVEDT†
*Institute for the Study of Earth, Oceans, & Space, 39 College Road, University of New Hampshire, Durham, NH 03824, USA, †CICERO, Center for International Climate and Environmental Research – Oslo, PO Box 1129, Blindern, 0318 Oslo, Norway

Abstract

Fertilized rice paddy soils emit methane while flooded, emit nitrous oxide during flooding and draining transitions, and can be a source or sink of carbon dioxide. Changing water management of rice paddies can affect net emissions of all three of these greenhouse gases. We used denitrification–decomposition (DNDC), a process-based biogeochemistry model, to evaluate the annual emissions of CH_4, N_2O, and CO_2 for continuously flooded, single-, double-, and triple-cropped rice (three baseline scenarios), and in further simulations, the change in emissions with changing water management to midseason draining of the paddies, and to alternating crops of midseason drained rice and upland crops (two alternatives for each baseline scenario). We used a set of first-order atmospheric models to track the atmospheric burden of each gas over 500 years. We evaluated the dynamics of the radiative forcing due to the changes in emissions of CH_4, N_2O, and CO_2 (alternative minus baseline), and compared these with standard calculations of CO_2-equivalent emissions using global warming potentials (GWPs). All alternative scenarios had lower CH_4 emissions and higher N_2O emissions than their corresponding baseline cases, and all but one sequestered carbon in the soil more slowly. Because of differences in emissions, in radiative forcing per molecule, and in atmospheric time constants (lifetimes), the relative radiative impacts of CH_4, N_2O, and CO_2 varied over the 500-year simulations. In three of the six cases, the initial change in radiative forcing was dominated by reduced CH_4 emissions (i.e. a cooling for the first few decades); in five of the six cases, the long-term radiative forcing was dominated by increased N_2O emissions (i.e. a warming over several centuries). The overall complexity of the radiative forcing response to changing water management could not easily be captured with conventional GWP calculations.

Key words: biogeochemistry, climate change, global warming potential, GWP, modeling

Received 9 September 2003; revised version received and accepted 23 December 2003

Introduction

The 1992 UN Framework Convention on Climate Change formally raised the issue of stabilizing the atmospheric concentrations of greenhouse gases to limit potential future hazards. In 1997, the Kyoto Protocol set a target for a suite of greenhouse gases: carbon dioxide (CO_2), methane (CH_4), nitrous oxide (N_2O), hydrofluorocarbons (HFCs), perfluorocarbons (PFCs), and sulfur hexafluoride (SF_6), evaluated as 'carbon dioxide equivalent emissions' (Art. 3.1., Annex A). This has generated discussion and research activity within the scientific community about assessing greenhouse gas emissions from various sectors of the human economy and from a range of terrestrial and aquatic ecosystems (e.g. Mosier *et al*., 1998; Seitzinger & Kroeze, 1998; Sass *et al*., 1999; Smith *et al*., 2000a, b; US EPA, 2002). Another area of ongoing research has been concerned with developing mechanisms for comparing the different greenhouse gases on a common basis (e.g. Lashof & Ahuja, 1990; Harvey, 1993; O'Neill, 2000; Smith & Wigley, 2000a, b; Fuglestvedt *et al*., 2003). Though there is a clear overlap between these two

Correspondence: Steve Frolking, tel. + 1 603 862 0244, fax + 1 603 862 0188, e-mail: steve.Frolking@unh.edu

subdisciplines of global change studies, most papers fall clearly into one or the other. Greenhouse gas flux studies typically use a convenient multiplier to compare the impact of different greenhouse gases, without addressing the complexities of the comparison of impacts (e.g. Robertson *et al*., 2000; Smith *et al*., 2001), while global warming index studies typically consider a convenient pulse or slab (i.e. sustained and constant) emission scenario, without addressing the complexities of realistic emissions for likely management, policy, or ecological changes in some sector. In this paper, we address both issues together by simulating realistic changes in CO_2, CH_4, and N_2O emissions from rice paddy fields due to likely changes in management, and evaluate the evolving net radiative forcing associated with these changes in emissions over a 500-year time period.

Cultivated cropland is a significant contributor to the atmospheric budgets of several greenhouse gases. Rice paddy fields emit about $50\,Tg\,CH_4\,yr^{-1}$ (Sass *et al*., 1999), roughly 10% of total global CH_4 emissions (Prather *et al*., 2001). Fertilized cropland soils emit about $2\,Tg\,N_2O\text{-}N\,yr^{-1}$, roughly 10% of total global N_2O emissions (Mosier *et al*., 1998). Over the first several decades of cultivation, soils typically lose about 10–50% of their organic carbon content (e.g. Davidson & Ackerman, 1993), and this is estimated to have contributed about $40\,Pg\,CO_2\text{-}C$ to the atmosphere over the past 150 years (Houghton, 2000).

As highly managed systems, croplands are likely targets for greenhouse gas mitigation actions (e.g. Oenema *et al*., 2001). Potential mitigation strategies in cropland cultivation are carbon sequestration in cropland soils (e.g. Smith *et al*., 2000a, b; West & Post, 2002), improved fertilizer management to reduce N_2O losses (e.g. Matson *et al*., 1998), and improved paddy water management to reduce CH_4 emissions (e.g. Wassmann *et al*., 2000b). A change in agricultural management can affect the net flux of more than one greenhouse gas, and several recent studies have recognized the importance of simultaneously considering multiple gases when evaluating the potential climate impacts of agricultural management (e.g. Robertson *et al*., 2000; Smith *et al*., 2000a; Marland *et al*., 2003).

The concept of global warming potential (GWP) was introduced in order to compare the climate impacts of emissions of different greenhouse gases (Lashof & Ahuja, 1990; Shine *et al*., 1990). CO_2 is typically taken as the reference gas, and an increase or reduction in emission of another greenhouse gas is converted into 'CO_2-equivalents' by means of its GWP, a multiplicative factor. In this way, it is possible to directly compare changes in non-CO_2 greenhouse gases with each other and with CO_2 (e.g. Robertson *et al*., 2000), and to compare the global warming impact of management scenarios for different economic sectors like agriculture and energy.

The GWP concept is designed to address potential climatic impact, and it is defined as a measure of the time-integrated radiative forcing due to a small pulse input of a greenhouse gas, where the time integration is over a specified time horizon. For a unit mass pulse input of greenhouse gas X, the GWP for a reference time horizon t is defined as (Ramaswamy *et al*., 2001)

$$\mathrm{GWP}_x^t = \frac{\int_0^t A_x[r_x(t)]\,\mathrm{d}t}{\int_0^t A_{\mathrm{CO_2}}[r_{\mathrm{CO_2}}(t)]\,\mathrm{d}t}, \tag{1}$$

where A is the radiative forcing per unit concentration (or mass) of gas X (A_x) or the reference gas, A_{CO2}, and $r(t)$ is the response function or decay in concentration of X or CO_2 following a pulse input at $t = 0$. The numerator of this equation is the absolute GWP for gas X and time horizon t (i.e. the integral sum of the instantaneous radiative forcing of gas X over the time horizon t, accounting for its changing (decaying) concentration in the atmosphere). Our concern in this study is with CO_2, CH_4, and N_2O, all of which are relatively well mixed in the atmosphere. The behavior of a pulse input of CH_4 and N_2O into the atmosphere is adequately represented by a first-order decay in concentration with a constant lifetime/adjustment time, τ, so the concentration is $r_x(t) = \exp(-t/\tau_x)$. Accurately portraying CO_2's lifetime/adjustment time in the atmosphere is more complicated, and can be approximated as the linear superposition of five first-order decay pools with different time constants, τ_i, and fractional contributions, α_i, (Table 1; Joos *et al*., 1996; Shine *et al*., 2004):

$$r_{\mathrm{CO_2}}(t) \sim \sum_{i=0}^{4} \alpha_i \exp(-t/\tau_i). \tag{2}$$

The assumption underlying the application of GWPs is that for a given time horizon t, an equivalent CO_2 pulse emission, ΔE^t_{CO2}, for a pulse emission of gas X, ΔE_x, is given by

$$\Delta E^t_{\mathrm{CO_2}} = \mathrm{GWP}^t_{\mathrm{x}} \cdot \Delta E_{\mathrm{x}}. \tag{3}$$

This equivalent CO_2 emission would produce the same integrated (to time t) radiative forcing as the emission of X. While the Intergovernmental Panel on Climate Change (IPCC) has defined GWPs for pulses of emissions, GWPs or alternatives may also be based on sustained emission changes (e.g. Fuglestvedt *et al*., 1996; Johnson & Derwent, 1996; Shine *et al*., 2004).

In this study, we investigated the greenhouse gas and climate forcing impacts of changing water management in rice paddy agriculture. Rice is the major food crop for much of Asia, grown on about 130 million hectares

Table 1 Greenhouse gas parameters

Gas	Radiative efficiency* (10^{-13} W m^{-2} kg^{-1})	Index†	Fraction‡	Time constant§ (years)	Indirect effects multiplier*
CO_2	0.0198	0	0.176	Infinite¶	1.0
	0.0198	1	0.138	421.0	1.0
	0.0198	2	0.186	70.6	1.0
	0.0198	3	0.242	21.4	1.0
	0.0198	4	0.259	3.42	1.0
CH_4	1.30	5	1.0	12.0	1.3
N_2O	3.96	6	1.0	113.0	1.0

*Ramaswamy *et al*. (2001).
†See Eqns (2) and (4) in the text.
‡CO_2 fraction values (α_i in Eqn (2)) are from Joos *et al*. (1996).
§CO_2 lifetimes/adjustment times (α_i in Eqn (2)) are from Joos *et al*. (1996); CH_4 and N_2O lifetimes/adjustment times are from Prather *et al*. (2001).
¶Modeled as 10^8 years.

(Maclean *et al*., 2002). Through a combination of expanded area and increased yield, rice production has roughly quadrupled since 1950, and demand is expected to increase by about 1% yr^{-1} for the next several decades (Maclean *et al*., 2002). About 60% of Asia's rice area is irrigated (Huke & Huke, 1997). Water management practices for irrigated rice have been changing in China from continuous flooding to midseason draining/drying, in which the field is allowed to dry slightly by reducing water inputs or is actively drained (Li *et al*., 2002). Agriculture currently accounts for about 85% of water withdrawals in Asia (International Rice Research Institute, 2002), but there is a continually increasing demand for water resources from industrial and municipal sectors (e.g. Vörösmarty *et al*., 2000). Thus, it is likely that paddy water management is or will be changing throughout much of Asia in the coming decades (Maclean *et al*., 2002).

Continuously flooded (CF) rice paddies are generally strong CH_4 sources throughout the growing season. Field studies have shown that midseason draining reduces total crop-season CH_4 emissions by 10–80% (Sass *et al*., 1992; Yagi *et al*., 1996; Cai *et al*., 1999; Wassmann *et al*., 2000a). N_2O emissions are generally quite low while the paddies are flooded, but midseason draining appears to cause an increase in N_2O emissions, with an emission pulse occurring most times the paddy soils dry slightly (Zheng *et al*., 1997; Cai *et al*., 1999). Changing water management may influence soil organic matter decomposition rates and also crop yield and, therefore, crop litter inputs to the soil, changing the net soil carbon balance, and thus site CO_2 balance. Thus, changing paddy water management, which is likely to occur either as a CH_4 emission mitigation strategy or because of water resource constraints, can change the net emissions of CO_2, CH_4, and N_2O from paddy fields. Changing paddy water management does not generate a single pulse emission perturbation, but rather a nonconstant change in net emissions of CO_2, CH_4, and N_2O. As a result, GWP calculations are inadequate for fully understanding the consequences of the changes in greenhouse gas emissions resulting from changing paddy water management. Alternative formulations of GWP or other indices that are based on sustained emission changes will also be inadequate since not all of the greenhouse gas emission changes are pulses, or sustained steps, but instead go through a transition period and ramp toward a sustained new emission level. In this study, we use the denitrification–decomposition (DNDC) agro-ecosystem biogeochemistry model to simulate a 550-year time series of net annual CO_2, CH_4, and N_2O fluxes from paddy fields under different agricultural management scenarios and for different sites. These net emissions are then used as the input for a simple atmospheric box model to determine the impact on atmospheric concentrations/burdens, and these concentrations/burdens are used to calculate the radiative forcing each year.

Methods

Emissions estimates

We used the DNDC model (Li *et al*., 1992) to simulate greenhouse gas emissions (CO_2, CH_4, N_2O). DNDC is a process-based agro-ecosystem model, consisting of two components to reflect the two-level driving forces that control C and N dynamics. The first component, which consists of soil climate, crop growth, and decomposition submodels, predicts soil profiles of temperature, moisture, pH, redox potential (Eh), and substrate concentration (e.g. dissolved organic carbon, mineral N, etc.), based on ecological and biophysical drivers (e.g. climate, soil, vegetation, and anthropogenic activity). The second component, which consists of nitrification, denitrification, and fermentation submodels, predicts NO, N_2O, N_2, CO_2, CH_4, and NH_3 gaseous fluxes based on the soil environmental variables. Classical laws of physics, chemistry, and biology, and empirical equations generated from laboratory observations, were used to parameterize each specific reaction (Li *et al*., 1992, 1994; Li, 2000; Zhang *et al*., 2002). Incorporation of these fundamental processes in DNDC has enabled the model to predict crop development/growth/yield, as well as soil C and N cycles including trace gas emissions driven by a limited number of well-documented drivers such as weather, soil properties, and farm management.

Due to the limited availability of field datasets, long-term (30–150 years) validation of DNDC has been done only for soil organic carbon (SOC) dynamics (Li *et al*., 1992, 1994; Smith *et al*., 1997). Tests of simulated CH_4 and N_2O fluxes are based on field studies that were typically 1 year or shorter (Li *et al*., 1992, 2002, 2003; Frolking *et al*., 1998; Li, 2000; Brown *et al*., 2002; Smith *et al*., 2002; Cai *et al*., 2003; Grant *et al*., 2004), including two comparisons with measurements in East Asia (Li *et al*., 2002; Cai *et al*., 2003). The reliability of long-term simulations of CH_4 and N_2O fluxes relies on the modeled relationships between N_2O and SOC, or between CH_4 and SOC, soil texture, and crop biomass.

In this study, we simulated three different rice paddy crop rotations in each of three different climatic zones (Table 2). The northern site, in Liaoning Province, China, had a single crop per year; the central site, in Jiangsu Province, China, had two crops per year, and the southern site, in Prachin, Thailand, had three crops per year. The three different crop-rotation scenarios simulated at each site represented a range in water management: CF rice for each crop, midseason drained rice (MSD) for each crop, and MSD rice alternating with nonirrigated upland crops (upland crop rotation or UCR) (Table 3). Note that in our scenarios, CF rice is flooded during the entire crop growth period, but is not flooded during any fallow periods.

We chose representative soil texture (clay percent) values for the three sites, with clay content increasing from north to south (Table 2); soil pH decreased from north to south, based on general trends in East Asia. SOC content was initialized at $0.015\,\mathrm{kg\,C\,kg^{-1}}$ soil for all sites; bulk density was set at $1.25\,\mathrm{g\,cm^{-3}}$ for all sites. Previous rice paddy simulations with DNDC have shown that soil texture has a strong influence on CH_4 emissions (Li *et al*., 2002; see also Sass *et al*., 1994), and other DNDC simulations (e.g. Li *et al*., 2001) have shown that SOC content has a strong influence on N_2O emissions. Daily weather data to drive the simulations for each site (daily precipitation and maximum and minimum air temperature) were taken from records from nearby meteorological station data; for the two sites in China, we used 1990 weather data; for the site in Thailand we used 1996 weather data. All of the climate/soil conditions used for this analysis were representative of Asian rice areas, but spanned a fairly conservative range; there would be many locations with soil properties or climate conditions outside the ranges used. With these input parameters, we expected the results to reflect general trends in behavior, although they are not likely to span the entire range of possible behaviors for a region as large as the rice-producing area of Asia.

Although crop management can change in many ways over a 500 year period, in this analysis we evaluated only the impact of changing water management on net fluxes of CO_2, CH_4, and N_2O across a range of climate and soil texture conditions representative of rice agriculture in Asia. Each simulation began with 50 years of CF rice, followed by 500 years of either CF rice, 500 years of MSD rice, or 500 years of MSD rice alternating with nonflooded crops (UCR). All other management factors (see Table 3 footnotes) were constant across all sites and all crop-rotation scenarios.

Table 2 Site characteristics

Site	Location	Latitude (°N)	MAT* (°C)	AP† ($\mathrm{mm\,yr^{-1}}$)	Crops ($\mathrm{yr^{-1}}$)	Soil clay content (%)	pH	Bulk density ($\mathrm{g\,cm^{-3}}$)	SOC_{init}‡ ($\mathrm{kg\,C\,kg^{-1}}$)
1	Liaoning, China	41.7	9.0	640	1	34	7.0	1.25	0.015
2	Jiangsu, China	32.5	17	900	2	49	6.5	1.25	0.015
3	Prachin, Thailand	13.9	29	1500	3	63	6.0	1.25	0.015

*MAT, mean annual air temperature for simulation.
†AP, annual precipitation for simulation.
‡Soil organic carbon in top 10 cm of soil at start of 550-year simulation.

Table 3 Simulation sites and agricultural management scenarios

Management scenarios*		SOC_{init} ($t\,C\,ha^{-1}$)	SOC_{final} ($t\,C\,ha^{-1}$)
1-CF	CF single-cropped rice	62	110
1-MSD	MSD single-cropped rice	62	100
1-UCR	Alternating MSD single rice and maize	62	96
2-CF	CF double-cropped rice	63	190
2-MSD	MSD double-cropped rice	63	180
2-UCR	MSD rice/winter wheat (double-cropped)	63	150
3-CF	CF triple-cropped rice	63	250
3-MSD	MSD triple-cropped rice	63	270
3-UCR	MSD rice/maize/vegetable (triple-cropped)	63	120

*CF, continuously flooded from day of transplanting to 10 days before harvest.
MSD, midseason drying with three drainings; flooded on day of transplanting, drained after 20 days, allowed to dry for 10 days, reflooded for 20 days, drained and allowed to dry for 10 days, reflooded for 20 days, drained and allowed to dry for 10 days, and reflooded again until 10 days before harvest. Additional management factors, common to all sites:

- N-fertilizer (urea) applied at rate of $100\,kg\,N\,ha^{-1}$ 4 weeks after planting of each crop.
- Farmyard manure (C : N = 13) applied at $1000\,kg\,C\,ha^{-1}\,yr^{-1}$;
- No irrigation applied to non-rice crops;
- tillage to 20 cm 2 days before seeding and to 10 cm just after harvest for each crop;
- 85% of postharvest above-ground crop residue removed from field.

The simulations were continued for 500 years after the management change to facilitate comparison with the standard GWP calculation with a 500-year time horizon.

We summed the simulated daily emissions of CH_4 and N_2O to determine annual emissions for each scenario. We calculated the annual change in SOC (ΔSOC) as end-of-year (31-Dec) minus beginning-of-year (1-Jan) values. SOC inputs were farmyard manure ($1000\,kg\,C\,ha^{-1}\,yr^{-1}$ for all scenarios) plus 15% of above-ground, nongrain crop biomass and 100% of below-ground crop biomass (i.e. crop residue that remains on site). We consider ΔSOC as net site annual CO_2 flux. CH_4 flux is another pathway for carbon out of wetland soil, but the primary substrates for CH_4 production are mainly plant-derived C (e.g. root exudation, deposition, and respiration CO_2) (Watanabe *et al.*, 1999; King *et al.*, 2002; Lu *et al.*, 2002), which are not included in the simulation SOC budget, so CH_4 flux would only be a small fraction of simulated ΔSOC.

Radiative forcing comparisons

The initial SOC values were not in equilibrium with the management practices applied in the simulations (primarily because of the application of $1000\,kg\,ha^{-1}\,yr^{-1}$ of farmyard manure), so site SOC values changed over the base-run simulation (discussed below in the results section). This caused non-steady-state emissions of CO_2 and N_2O for all simulations, with emission rates generally approaching equilibrium by the end of the simulation. Since our analysis was focused on the impact of changing water and crop-rotation management, with continuous flooding as the baseline or 'standard practice', we calculated annual CO_2, CH_4, and N_2O flux differentials as the MSD or UCR annual flux minus the CF annual flux, called MSD−CF and UCR−CF. These annual flux differentials were the input perturbation to the atmosphere that caused a net radiative forcing.

In a manner analogous to the GWP approach, we modeled the atmospheric burden of CH_4 and N_2O as single reservoirs with an annual input (the annual CH_4, or N_2O flux differential, Φ_i, which could be positive or negative) and a first-order loss (reservoir mass divided by constant reservoir lifetime/adjustment time, Table 1). The atmospheric concentration of CO_2 was modeled as a collection of five noninteracting global reservoirs, each with an annual input equal to the annual CO_2 flux differential multiplied by the reservoir fraction (Table 1) and a first-order loss determined by the reservoir lifetime (Table 1; Joos *et al.*, 1996; Shine *et al.*, 2004). The model integration used a fourth-order Runga–Kutta method, applied at an annual time step, resulting in annual CO_2, CH_4, and N_2O burden differences from background. Radiative forcings (again, positive or negative) due to the flux perturbations were then calculated each year as the product of each reservoir mass times the gas's radiative forcing factor (Table 1). The total radiative forcing, RF_{total}, was calculated as the sum of the individual gas contributions, and can be written as

$$RF_{total}(t) = \sum_{i=0}^{6}\left(\xi_i A_i f_i \int_0^t \Phi_i(t')e^{(t'-t)/\tau_i}dt'\right), \quad (4)$$

where ξ_i is a multiplier for indirect effects (Table 1), A_i is the radiative efficiency of the greenhouse gas i (Table 1), f_i is the fractional multiplier for the flux of the greenhouse gas i (Table 1), and $\Phi_i(t')$ is the simulated flux differential of greenhouse gas i at time t'. Note that CO_2 is the greenhouse gas for $i = 0$–4 (Table 1). This methodology assumed that the flux perturbations (positive or negative) were small compared with the global atmospheric burdens of CO_2, CH_4, and N_2O, and that a linear radiative forcing response to the perturbations was a good approximation, even over long time periods. We tested the model by forcing it with single-pulse emissions of CO_2, CH_4, and N_2O, each weighted by the inverse of the 100-year GWP value (1.0 for CO_2, by definition; 23 for CH_4; and 292 for N_2O; Ramaswamy *et al.*, 2001). We then summed the annual radiative forcing for each gas predicted by the atmospheric model; all three gases generated the same integrated radiative forcing at 100 years, establishing that the model is consistent with the GWP calculations in Eqn (3). However, the model goes beyond the standard GWP calculation by (1) allowing for a nonpulse and non-constant input, and (2) providing the instantaneous radiative forcing for each year of the simulation. By converting changing emissions rates of CO_2, CH_4, and N_2O into atmospheric forcing (e.g. $\mathrm{mW\,m^{-2}}$) the three gases can all be compared in common units, and the total effect can be quantified.

Finally, the radiative forcing caused by the CO_2, CH_4, and N_2O flux differentials was compared with the radiative forcing of a constant equivalent amount of CO_2 emissions for a fixed time period in order to assess the accuracy of the GWP method for comparison of emissions. These equivalent CO_2 emissions were calculated using 20-, 100-, and 500-year mean flux differentials for each gas. For example, $\langle CH_4\rangle_{20}^{1-\mathrm{MSD}}$ is the difference between the mean CH_4 flux in scenario 1-MSD and scenario 1-CF for the first 20 simulation years (Table 4). For this case, the 20-year time horizon CO_2-equivalent flux differential (Table 5) is calculated as

$$\begin{aligned}(CO_{2\text{-eq.}})_{20} &= [CO_2\ \text{flux}] + [\text{methane}\ CO_2\text{-equivalent}] \\ &\quad + [\text{nitrous oxide}\ CO_2\text{-equivalent}] \\ &= \langle CO_2\rangle_{20}^{1-\mathrm{MSD}} \times \frac{44}{12} \\ &\quad + \langle CH_4\rangle_{20}^{1-\mathrm{MSD}} \times \frac{16}{12} \times \mathrm{GWP}_{20}^{CH_4} \\ &\quad + \langle N_2O\rangle_{20}^{1-\mathrm{MSD}} \times \frac{44}{28} \times \mathrm{GWP}_{20}^{N_2O},\end{aligned} \tag{5}$$

where the numerical fractions are the ratios of molecular weights (CO_2, CH_4, and N_2O) to elemental weights (C and N). This CO_2-equivalent flux differential was then used as an atmospheric perturbation input for 20 years, and then the CO_2 input was set to zero and the atmosphere continued to evolve for the remaining 480 years of the simulation. Equivalent calculations were done for all scenario changes and for each of the time horizons (Table 5). As an atmospheric input, each 100-year time horizon CO_2-equivalent flux lasted for 100 years, and each 500-year time horizon CO_2-equivalent flux lasted for 500 years. The atmospheric concentration and radiative forcing response was calculated with the same model (Eqn (4)). In all cases, the CO_2-equivalent radiative forcing rate increased monotonically for the duration of the CO_2 inputs and then decreased monotonically after that, based on the time constants of the five atmospheric CO_2 pools (Table 1).

Results

Emissions estimates

Base-run simulations of CF rice. The Liaoning site base-run simulation (CF single rice) initially accumulated SOC at a rate of about $600\,\mathrm{kg\,C\,ha^{-1}\,yr^{-1}}$, but approached equilibrium ($\Delta\mathrm{SOC} < 20\,\mathrm{kg\,C\,ha^{-1}\,yr^{-1}}$) after about 200 years (Fig. 1a). SOC accumulation was due to the soil coming into equilibrium as inputs (manure and crop residue) matched outputs (decomposition). Higher SOC caused increasing N_2O fluxes, which rose from about 9 to about $19\,\mathrm{kg\,N_2O\text{-}N\,ha^{-1}\,yr^{-1}}$ over the first 120 years of the simulation. Annual CH_4 flux was approximately constant at a high rate of about $120\,\mathrm{kg\,CH_4\text{-}C\,ha^{-1}\,yr^{-1}}$ over the entire simulation.

The Jiangsu site base-run simulation (CF double rice) initially accumulated SOC at a rate of about $1200\,\mathrm{kg\,C\,ha^{-1}\,yr^{-1}}$, and approached equilibrium ($\Delta\mathrm{SOC} < 50\,\mathrm{kg\,C\,ha^{-1}\,yr^{-1}}$) by the end of the simulation (Fig. 1b). Again, SOC accumulation was due to the soil coming into equilibrium, driven by the crop carbon cycle and manure inputs of the prescribed management. Increasing SOC content caused N_2O fluxes to rise from about $3\,\mathrm{kg\,N_2O\text{-}N\,ha^{-1}\,yr^{-1}}$ to a quasisteady value of about $8\,\mathrm{kg\,N_2O\text{-}N\,ha^{-1}\,yr^{-1}}$ over the first 200 years of the simulation. Annual CH_4 flux was approximately constant at about $100\,\mathrm{kg\,CH_4\text{-}C\,ha^{-1}\,yr^{-1}}$ over the entire simulation.

The Thailand site base-run simulation (CF triple rice) initially accumulated SOC at a rate of about $1300\,\mathrm{kg\,C\,ha^{-1}\,yr^{-1}}$, and was approaching equilibrium ($\Delta\mathrm{SOC} \sim 100\,\mathrm{kg\,C\,ha^{-1}\,yr^{-1}}$ by the end of the simulation) (Fig. 1c). Higher SOC content caused increasing N_2O fluxes, initially about $5.0\,\mathrm{kg\,N_2O\text{-}N\,ha^{-1}\,yr^{-1}}$ and approaching equilibrium at about $24\,\mathrm{kg\,N_2O\text{-}N\,ha^{-1}\,yr^{-1}}$ by the end of the simulation. Annual CH_4 flux was

Table 4 Mean annual greenhouse gas emissions for simulation years 51–70 (20 years), 51–150 (100 years), and 51–550 (500 years)

	CO_2[†]			CH_4			N_2O		
Management scenario*	20 years	100 years	500 years	20 years	100 years	500 years	20 years	100 years	500 years
1-CF	−210.0	−140.0	−58.0	120.0	120.0	120.0	16.0	18.0	17.0
1-MSD	−75.0	−66.0	−33.0	53.0	53.0	52.0	23.0	25.0	24.0
1-UCR	180.0	11.0	−27.0	25.0	25.0	25.0	17.0	17.0	15.0
2-CF	−470.0	−350.0	−160.0	110.0	110.0	100.0	4.0	5.7	7.2
2-MSD	−320.0	−250.0	−130.0	64.0	64.0	63.0	20.0	25.0	29.0
2-UCR	430.0	5.0	−71.0	35.0	35.0	33.0	20.0	25.0	29.0
3-CF	−730.0	−590.0	−280.0	210.0	210.0	210.0	15.0	18.0	22.0
3-MSD	−730.0	−640.0	−320.0	140.0	140.0	140.0	50.0	58.0	68.0
3-UCR	410.0	32.0	−22.0	36.0	36.0	36.0	45.0	47.0	48.0

CO_2 and CH_4 in $kg\,C\,ha^{-1}\,yr^{-1}$; N_2O in $kg\,N\,ha^{-1}\,yr^{-1}$. All values reported to two significant figures.
*See Table 3 for details.
[†]CO_2 flux is equal to annual change in soil organic carbon (negative value means net C sequestration in soil).

Table 5 Equivalent CO_2 emissions ($kg\,CO_{2\text{-eq}}\,ha^{-1}\,yr^{-1}$) for flux differentials due to changes in management for 20-, 100-, and 500-year time horizons

	CO_2			CH_4			N_2O			Total[†]		
Scenario change*	20 years	100 years	500 years	20 years	100 years	500 years	20 years	100 years	500 years	20 years	100 years	500 years
GWP value[‡] →	1	1	1	62	23	7	275	296	156			
1-MSD – 1-CF	500	270	92	−5500	−2100	−650	3000	3200	1800	−2100	1300	1200
1-UCR – 1-CF	1500	550	120	−7900	−2900	−900	430	−600	−390	−6000	−3000	−1200
2-MSD – 2-CF	540	360	100	−3400	−1300	−380	7000	8800	5300	4100	7900	5000
2-UCR – 2-CF	3300	1300	330	−5800	−2200	−660	7000	8800	5300	4500	7900	5000
3-MSD – 3-CF	−35	−180	−160	−6000	−2200	−670	15 000	18 000	11 000	9000	16 000	10 000
3-UCR – 3-CF	4200	2300	950	−15 000	−5500	−1700	13 000	14 000	6200	200	10 000	5500

All values reported to two significant figures. GWP, global warming potential.
*See Table 3 for details.
[†]See Eqn (5) in text; totals may not add due to round-off.
[‡]Ramaswamy *et al*. (2001).

approximately constant at about 210 $kg\,CH_4\text{-}C\,ha^{-1}\,yr^{-1}$ over the entire simulation.

In all cases, the initial SOC values were not in equilibrium with the management practices applied in the simulations, and site SOC values changed over the base-run simulations (Table 3), leading to changes in N_2O emissions (Table 4). In this study, we were not interested in changes in SOC, CH_4 flux, or N_2O flux resulting from the interaction between the prescribed management and site-specific initial conditions. Therefore, we evaluate only the differences in ΔSOC, CH_4 flux, and N_2O flux between the CF rice baseline (scenarios 1-CF, 2-CF, and 3-CF) and MSD rice (scenarios 1-MSD, 2-MSD, and 3-MSD), or MSD rice alternating with a nonirrigated crop (scenarios 1-UCR, 2-UCR, and 3-UCR). Evaluating these differentials eliminates the trends in gas fluxes due to the disequilibrium between initial SOC and the management regime, and instead highlights only differences due to management changes.

Impacts of changing water management – flux differentials. Midseason draining of paddies reduced CH_4 emissions by about 60% at the northern China site (scenario 1-MSD), and by about one-third at both the southern China site (scenario 2-MSD) and the Thailand site (scenario 3-MSD) (Fig. 2a, c, e; Table 4). Fields became a weak CH_4 sink (~1 $kg\,CH_4\text{-}C\,ha^{-1}\,yr^{-1}$) when planted to a nonirrigated upland crop. For scenario 1-UCR, this led to alternating years as a moderately strong source or weak sink of CH_4, reducing the long-term mean flux by half again (Fig. 2b; Table 4). For scenario 2-UCR, this

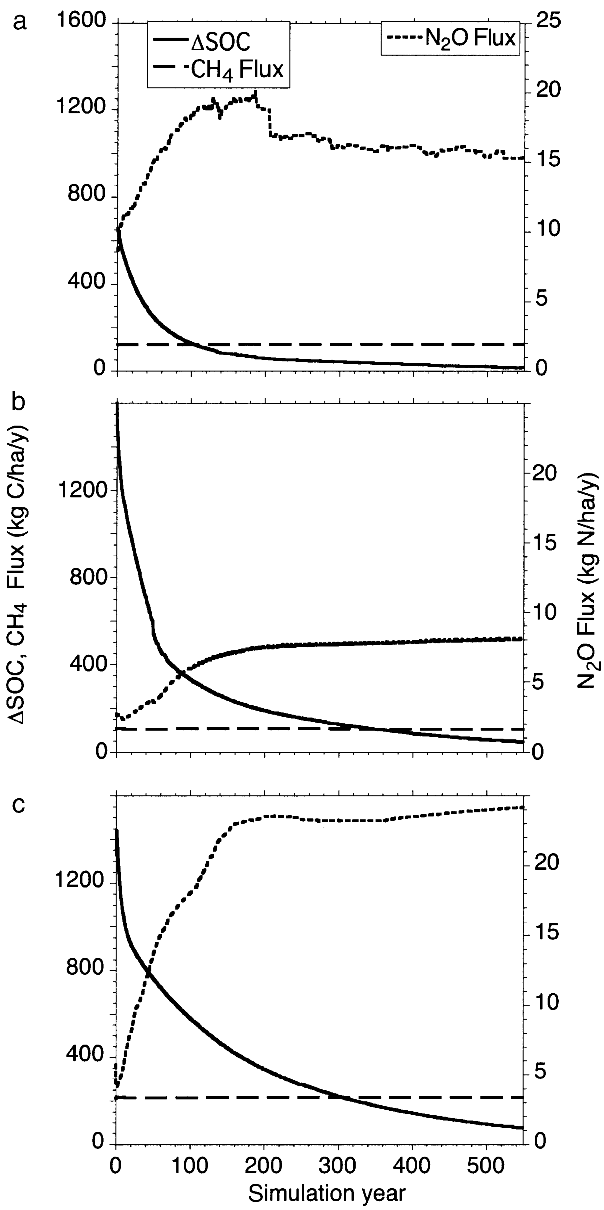

Fig. 1 Simulated change in soil organic carbon (SOC) (solid line, $kg\,C\,ha^{-1}\,yr^{-1}$), CH_4 flux (dashed line, $kg\,CH_4\text{-}C\,ha^{-1}\,yr^{-1}$), and N_2O flux (dotted line, $kg\,N_2O\text{-}N\,ha^{-1}\,yr^{-1}$) for the base-run scenarios (continuous flooding rice paddy) for (a) single rice in northern China, (b) double rice in southern China, and (c) triple rice in Thailand. In all cases, CH_4 fluxes are nearly constant over the 550-year simulation, SOC accumulation is initially high, but slowly drops toward zero, and N_2O flux increases, due to increasing SOC.

reduced CH_4 flux to about one-third of the CF value, and for scenario 3-UCR this reduced CH_4 flux to about 15% of the CF value.

Midseason draining of paddies increased N_2O emissions by about $7\,kg\,N_2O\text{-}N\,ha^{-1}\,yr^{-1}$ (or 40%) at the northern China site (scenario 1-MSD), by about $20\,kg\,N_2O\text{-}N\,ha^{-1}\,yr^{-1}$ (or 350%) at the southern China site (scenario 2-MSD), and by about $43\,kg\,N_2O\text{-}N\,ha^{-1}\,yr^{-1}$ (or 200%) at the Thailand site (scenario 3-MSD) (Fig. 2a, c, e; Table 4). At the northern China site, converting from CF double rice to alternate year MSD rice and nonirrigated maize decreased N_2O emissions by about $1\text{–}2\,kg\,N_2O\text{-}N\,ha^{-1}\,yr^{-1}$ (Fig. 2b; Table 5). At the southern China site, converting from CF double rice to MSD rice/winter wheat increased annual N_2O emissions by about $20\,kg\,N_2O\text{-}N\,ha^{-1}\,yr^{-1}$ (Fig. 2d; Table 4), the same as with the conversion to MSD double rice. At the Thailand site, converting from CF triple rice to MSD rice and maize and vegetable crops increased annual N_2O emissions by about $25\,kg\,N_2O\text{-}N\,ha^{-1}\,yr^{-1}$ (Fig. 2f; Table 4), about half the increase caused by the switch to MSD triple rice.

At the northern and southern China sites, conversion from CF rice to MSD rice initially reduced the rate of carbon sequestration in the soils by $\sim 150\,kg\,C\,ha^{-1}\,yr^{-1}$, but this gradually decreased to no significant differences in ΔSOC as both scenarios approached soil carbon equilibrium (Fig. 2a, c, Table 4). Conversion to the UCR rotation at the northern China site caused an alternating pattern in SOC (Fig. 2b) that lost more carbon during the aerobic maize year than it gained during the anaerobic rice year, with an overall slow loss of SOC (Table 4). For both the southern China site and the Thailand site, conversion to the UCR rotation crops caused a significant reduction in the initial rate of carbon sequestration, because the nonharvested biomass yield for vegetable crop was much less than for rice, so crop litter inputs to the soil were reduced (Fig. 2d, f); this made for a strong positive CO_2 flux differential. This difference relaxed toward zero over the course of the simulation. For the Thailand site, the conversion from CF to MSD triple rice caused a small increase in the rate of SOC sequestration (Fig. 2e).

Flux differential and atmospheric burden perturbations

The atmospheric lifetime/adjustment time of each gas (Table 1) determined the persistence of flux perturbations on atmospheric burdens (Fig. 3). In all scenarios, the methane burden perturbation reached an equilibrium value within about 50 years after the management conversion, while the N_2O burden perturbations generally approached equilibrium late in the 550-year simulation. The situation is more complex for carbon dioxide, both because the flux perturbation inputs started high and decayed to near zero (Fig. 2), and because atmospheric CO_2 was partitioned into five pools with different time constants (Table 1). The general pattern for most sites was for the perturbed atmospheric CO_2 burden to rise to a maximum, then to

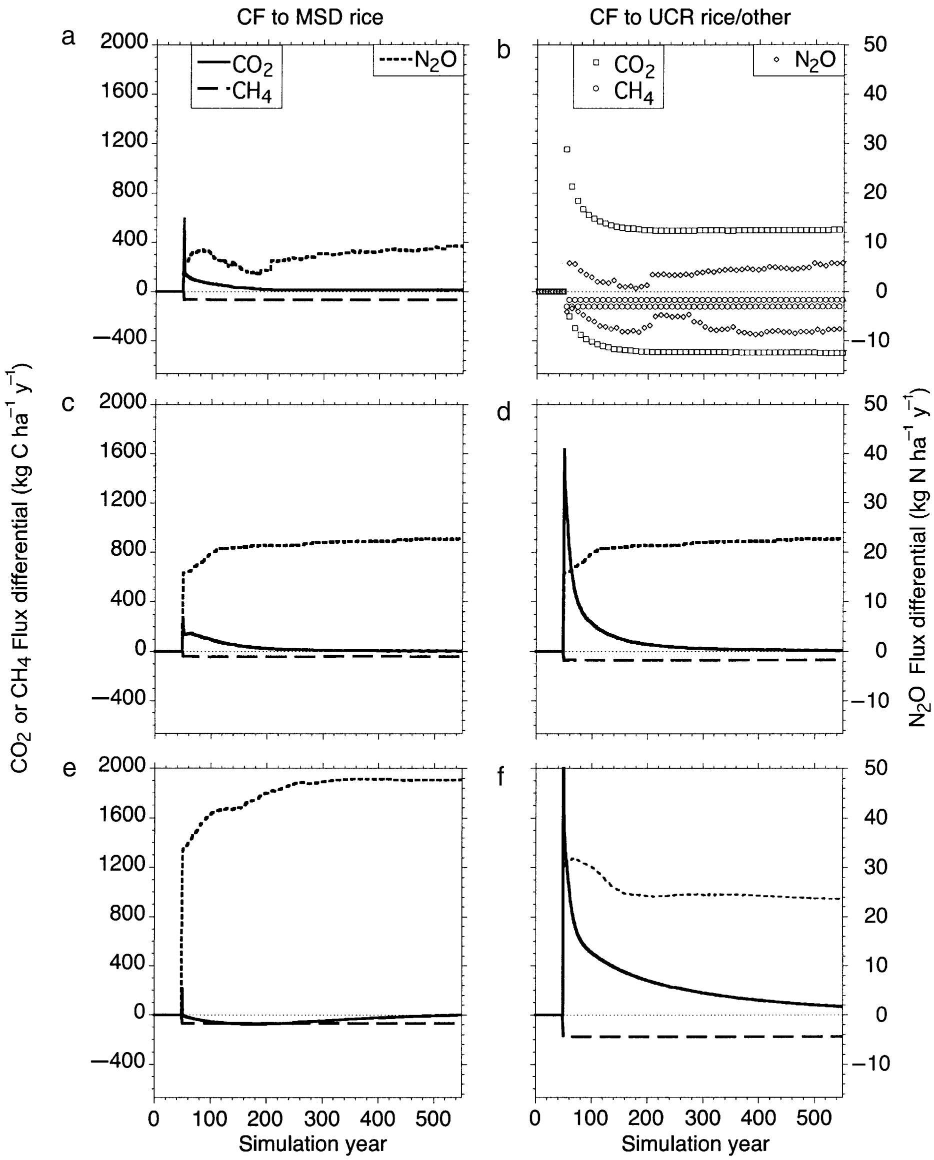

Figure 2 Simulated annual flux differentials of CO_2 (solid line, left axis, kg CO_2-C ha^{-1} yr^{-1}), CH_4 (dashed line, left axis, kg CH_4-C ha^{-1} yr^{-1}), and N_2O (dotted line, right axis, kg N_2O-N ha^{-1} yr^{-1}) at the northern China site for (a) MSD single rice and (b) alternate year MSD single rice and nonirrigated maize; at the southern China site for (c) MSD double rice and (d) MSD rice/nonirrigated winter wheat double cropping; and at the Thailand site for (e) MSD triple rice and (f) MSD rice/nonirrigated maize/nonirrigated vegetables triple cropping. Flux differentials equal the difference between the alternative water management (MSD in left column, UCR in right column) and baseline water management (CF); see text for details. Note that for the UCR in Liaoning Province (panel b), all fluxes oscillate between stable values or trends each year, as a single-rice crop alternates with a maize crop. The figure shows only every fifth year for clarity. A multiyear running mean of these oscillating values generates a steady CH_4 flux of about −95 kg CH_4-C ha^{-1} yr^{-1}, a steadily declining CO_2 flux that approaches zero within about 200 years, and a small N_2O flux of about −2 kg N_2O-N ha^{-1} yr^{-1}. The change in management began after 50 years, so the differentials were zero until year 50.

slowly relax toward a lower equilibrium value (Fig. 3b–f). The approach to equilibrium was slower as soil clay content increased. For the northern China site, where ΔSOC never fell to zero (Fig. 2a), this constant, small CO_2 flux differential caused the atmospheric burden perturbation to increase at a slow rate for the last 300 years of the simulation, after partially recovering from the initial pulse (Fig. 3a). Since, in the context of this model, one of the CO_2 pools has an infinite time constant, a CO_2 burden perturbation persisted even when the CO_2 flux perturbation had dropped to zero. Because of the integrating nature of atmospheric pools

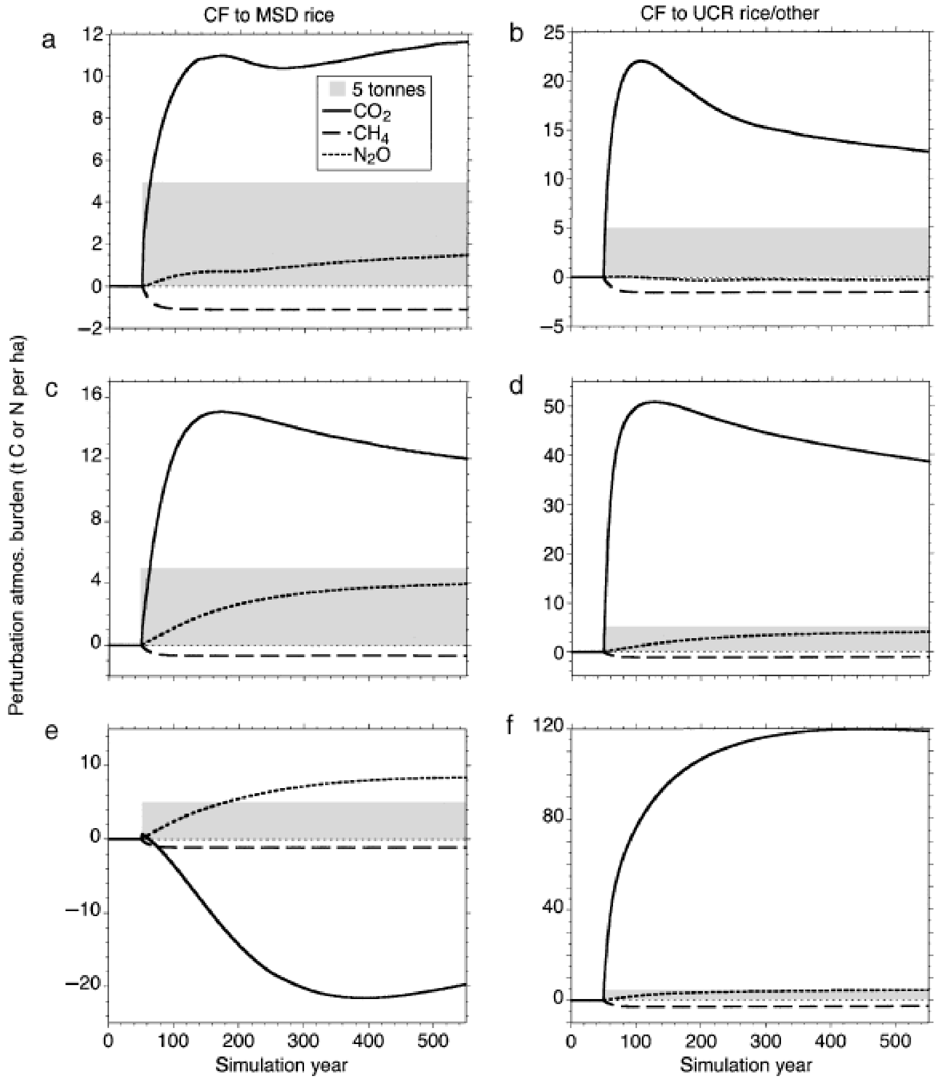

Figure 3 Simulated atmospheric burden perturbations of CO_2 (solid line), CH_4 (dashed line), and N_2O (dotted line) caused by changing management from continuously flooded (CF) single rice at the northern China site to (a) midseason drained (MSD) single rice and (b) alternate year MSD single rice and nonirrigated maize; from CF double rice at the southern China site to (c) MSD double rice and (d) MSD rice/nonirrigated winter wheat double cropping; from CF triple rice at the Thailand site to (e) MSD triple rice and (f) MSD rice/nonirrigated maize/nonirrigated vegetables triple cropping. Note: global atmospheric burden perturbations units are in tons CO_2-C, CH_4-C, or N_2O-N; this is the perturbation caused by a management change on 1 ha of paddy field. For comparison between cases, all panels have a gray-shaded region representing an atmospheric burden of +5 ton of C or N for years 50–550.

with long adjustment times, the response to a highly variable source (e.g. the N_2O perturbation for scenario 1-UCR) is a relatively smooth burden curve (Fig. 3b). In all cases, the absolute burden perturbation (in kilograms of gas) was greatest for CO_2; in all but the northern China UCR–CF case (Fig. 3b), CH_4 had the smallest absolute burden perturbation.

Flux differential radiative forcings

Multigas emissions. The simulated radiative forcing perturbation for each individual gas is directly proportional to its perturbation burden, based on the radiative efficiency of each gas (Table 1). For convenience, a positive radiative forcing perturbation is also called a warming, and a negative radiative forcing perturbation is called a cooling. For the northern China site, which had high CH_4 fluxes for a single-rice crop, the reduction in CH_4 emission with midseason draining and upland cropping (1-UCR scenario) was the dominant factor in the total radiative forcing, leading to an overall negative net radiative forcing (i.e. cooling effect; Fig. 4b). For the northern China site, conversion to MSD rice, the reduction in CH_4 emissions dominated the initial radiative forcing, causing a net cooling for the first 36 years, after which the increase in N_2O flux more than offsets the decrease in CH_4 flux (Fig. 4a). Similarly, for the Thailand site, conversion from CF rice to MSD rice alternating with upland maize and vegetables, the reduction in CH_4 emissions dominated the net radiative forcing for the first 13 years after conversion (Fig. 4f). In the other three cases, positive radiative forcing from N_2O was dominant, and there was an overall net warming for the entire period following conversion (Figs 4c,–e). In all cases, CO_2, with a relatively low radiative efficiency, had the smallest influence on the total radiative forcing. Its largest impact was in the Thailand site conversion from CF rice to MSD rice alternating with upland maize and vegetables, where replacing one of the rice crops with a vegetable crop with much lower crop residue to return to the soil reduced carbon inputs into the soil enough to make the net CO_2 balance (flux to atmosphere) large enough to offset about half the radiative impact of reduction in CH_4 emissions (Fig. 4f); N_2O was still the dominant greenhouse gas in this case.

Comparison with CO_2-equivalent emissions. Replacing the full multigas model with a constant, finite duration equivalent emissions of CO_2 ('Total' columns in Table 5)

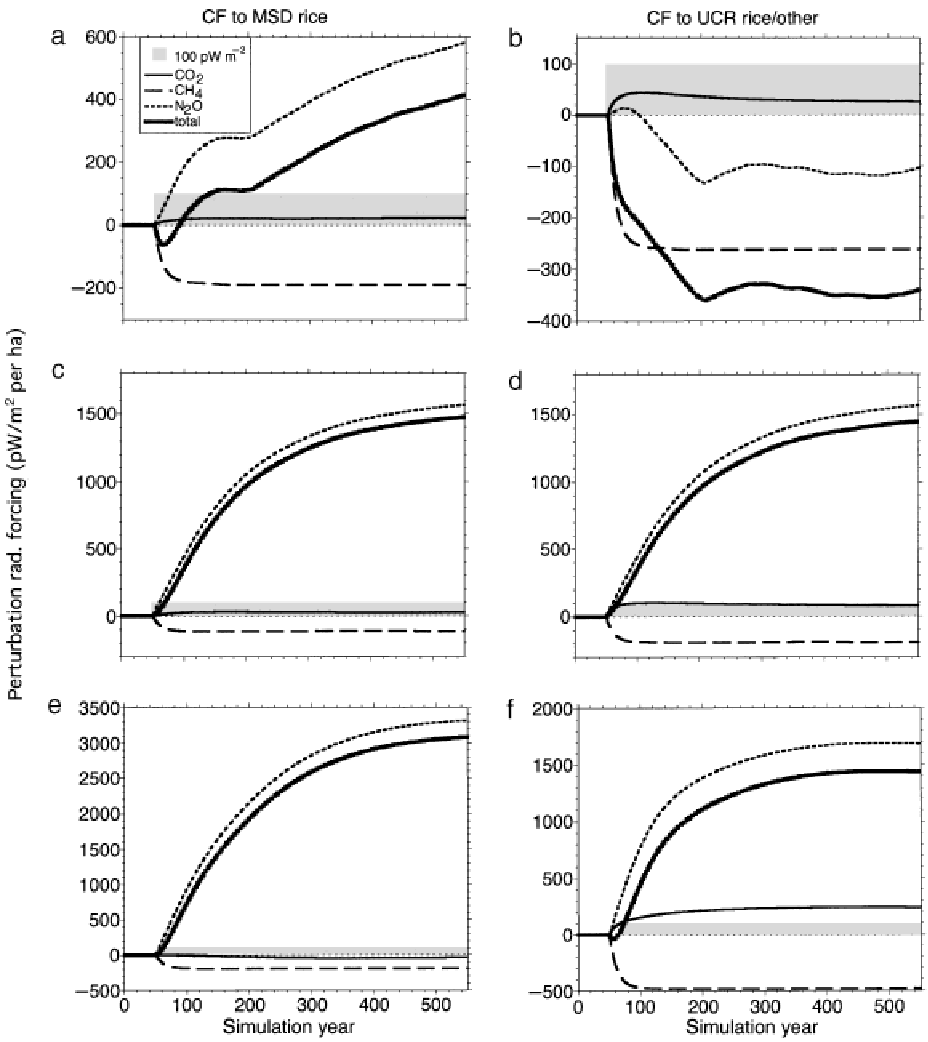

Fig. 4 Simulated radiative forcing each year due to CO_2 (solid line), CH_4 (dashed line), N_2O (dotted line), and all three gases (heavy solid line), based on burden perturbations in Fig. 3, due to changing management from continuously flooded (CF) single rice at the northern China site to (a) midseason drained (MSD) single rice and (b) alternate year MSD single rice and nonirrigated maize; from CF double rice at the southern China site to (c) MSD double rice and (d) MSD rice/nonirrigated winter wheat double cropping; from CF triple rice at the Thailand site to (e) MSD triple rice and (f) MSD rice/nonirrigated maize/nonirrigated vegetables triple cropping. Note: radiative forcing units are pW m^{-2}; this is the global radiative forcing caused by a management change on 1 ha of paddy field. For comparison between cases, all panels have a gray-shaded region representing a radiative forcing of $+100$ pW m^{-2} for years 50–550.

generated radiative forcings that approximated, to varying degrees, the full model behavior (Fig. 5). For the 20- and 100-year scenarios, once CO_2-equivalent emissions stopped (after 20 or 100 years), the radiative forcing slowly decayed to about half the peak value (Fig. 5), as the atmospheric CO_2 pools with shorter time constants (Table 1) decayed. The same behavior would occur in the 500-year scenario, if an additional 500 years were simulated. For the two scenarios with initial cooling but long-term warming, the 20-year CO_2-equivalent emissions reflects the initial cooling, and generates a weak cooling for the entire period, while the 100- and 500-year CO_2-equivalent emissions do not capture this initial cooling and instead reflect the long-term warming (Fig. 5a, f). In the scenarios with a smooth, monotonic net radiative forcing, the 20- and 100-year CO_2-equivalent emissions generated good approximations to the full model behavior for 20 and 100 years, respectively, while the 500-year CO_2-equivalent emissions underpredicted net radiative

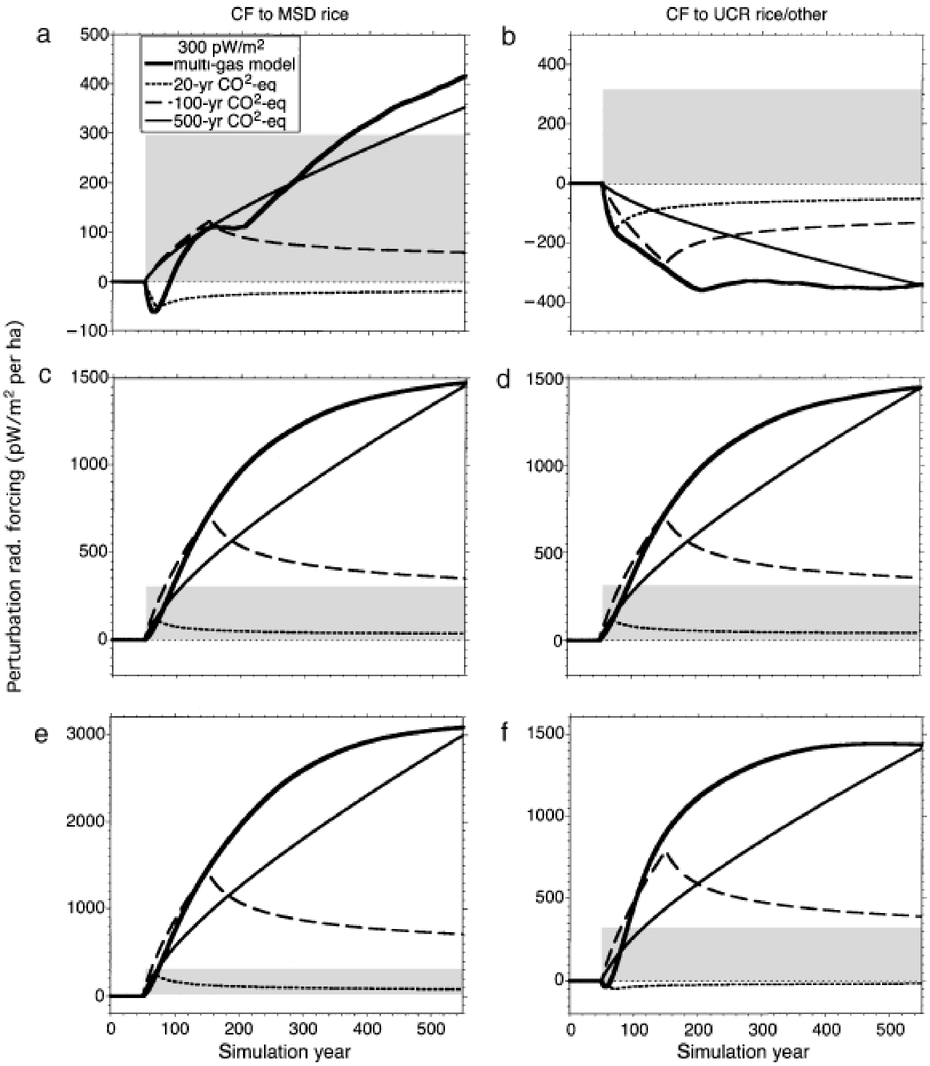

Fig. 5 Simulated total radiative forcing each year for the net greenhouse emissions due to changing management (heavy solid line; same as total radiative forcing line in Fig. 4), compared with total radiative forcing for constant GWP_{20} CO_2-eq emissions for 20 years (dotted line), constant GWP_{100} CO_2-eq emissions for 100 years (dashed line), and constant GWP_{500} CO_2-eq emissions for 500 years (solid line), for the northern China site to (a) MSD single rice and (b) alternate year MSD single rice and nonirrigated maize; from CF double rice at the southern China site to (c) MSD double rice and (d) MSD rice/nonirrigated winter wheat double cropping; from CF triple rice at the Thailand site to (e) MSD triple rice and (f) MSD rice/nonirrigated maize/nonirrigated vegetables triple cropping. See Table 5 for CO_2-equivalent flux rates. Note: radiative forcing units are $pW\,m^{-2}$; this is the global radiative forcing caused by a management change on 1 ha of paddy field. For comparison between cases, all panels have a gray-shaded region representing a radiative forcing of $+300\,pW\,m^{-2}$ for years 50–550.

forcing for most of the simulations (Fig. 5b–f). The discrepancy for the 500-year time horizon may be caused by the relationship between lifetimes/adjustment times and time horizon. The radiative forcing is dominated by N_2O and CH_4, both with adjustment times much less than 500 years, while about one-sixth of the CO_2-equivalent input has an adjustment time of 421 years and another sixth has an infinite adjustment time (Table 1). These longer adjustment times may lead to a lag in the radiative impact of the CO_2-equivalent emissions. If so, then the mix of gases will be an important factor in deciding which time horizon is most appropriate to reflect the emission changes. Transferring a suite of emission changes into 500-year CO_2-equivalent emissions may be a poor approximation if a large fraction of the gases have adjustment times much less than 500 years.

Discussion and conclusions

Gas flux results

The modeled CH_4 emissions for CF paddies (scenarios 1-CF, 2-CF, and 3-CF) ranged from 90 to 214 kg CH_4-C $ha^{-1}\,yr^{-1}$ (Fig. 1a–c, Table 4). The modeled range is within the reported CH_4 fluxes, which varied from 9 to 725 kg C $ha^{-1}\,yr^{-1}$ for China, and from 20 to 286 kg C $ha^{-1}\,yr^{-1}$ for Thailand (Cai *et al*., 2003). In addition, the modeled decrease in CH_4 emissions due to midseason drainage is supported by numerous observations (Yagi *et al*., 1990, 1996; Sass *et al*., 1992; Nugroho *et al*., 1994; Wassmann *et al*., 2000a). In this study, the DNDC-predicted mean N_2O emissions over the 550-year simulations from CF paddies (scenarios 1-CF, 2-CF, and 3-CF) ranged from 7.2 to 22 kg N_2O-N $ha^{-1}\,yr^{-1}$ (Fig. 1a–c, Table 4), with highest emissions at the warmest site, which also had three crops per year, and thus the highest N-fertilizer inputs and the most floodings and drainings (at the beginning and end of each rice crop season in CF cases). This result remains not validated due to the lack of multiyear, year-round measurements of N_2O emissions from rice paddies. However, the predicted positive relation between N_2O fluxes and SOC is supported by observations worldwide (e.g. Bouwman *et al*., 2002; Li *et al*., 2004). DNDC predicted increases in SOC under the flooded rice cultivations for all the three sites. The modeled trends are consistent with observations in the rice fields in China (Cai, 1996).

Changing paddy water management affects CH_4, N_2O, and CO_2 fluxes

Most analyses of greenhouse gas emission from rice paddies, and of possible greenhouse gas emission mitigation strategies, have focused on CH_4 (Wassmann *et al*., 2000b), and paddies are regularly listed as a category in global CH_4 budgets (e.g. Prather *et al*., 2001). Paddy soils have not been prominent in discussions of carbon sequestration in agricultural soils (e.g. Paustian *et al*., 2000; Smith *et al*., 2000a, b; West & Post, 2002) because these analyses have focused on Europe and North America, neither of which have large areas of rice paddies. N_2O emissions from CF paddies are low (e.g., Chen *et al*., 1995; Zheng *et al*., 1997; Cai *et al*., 1999) and there have been only a few published studies of increased N_2O fluxes with changing water management (Smith *et al*., 1982; Lindau *et al*., 1990; Zheng *et al*., 1997; Cai *et al*., 1999). In our analysis, we considered both short- and long-term impacts of emissions of CO_2, CH_4, and N_2O.

We first discuss the radiative impact of the mean long-term fluxes for the CF rice base case scenarios in terms of standard calculations of CO_2-equivalents based on GWP values. All three CF scenarios have relatively high CH_4 emissions and moderate N_2O emissions (Table 4). For a 20-year time horizon at all sites, the mean CH_4 flux is higher in terms of CO_2-equivalents than the mean N_2O flux; for a 100-year time horizon, mean CH_4 and mean N_2O fluxes have similar CO_2-equivalents; and, for a 500-year time horizon, the mean N_2O flux has higher CO_2-equivalents than the mean CH_4 flux (Table 6). Thus, targeting mitigation at reducing CH_4 and/or N_2O emissions depends on the time horizon chosen; the longer the time horizon, the more important N_2O emissions become.

In all cases, changing paddy water management from continuous flooding to midseason draining reduced CH_4 emissions by 30–50%, increased N_2O emissions by 100–500%, and had a relatively small effect on the rate of carbon sequestration (considered to represent net CO_2 flux) in the paddy soil (Table 4). In all cases, further reducing the amount of time a field was flooded by growing upland crops in place of some of the rice paddy crops caused a larger reduction in CH_4 emissions than just changing water management to midseason draining (Table 5). This effect was strongest for the triple-cropped site in Thailand. The impact on N_2O emissions of incorporating upland crops in the rotation was varied. For the northern China site, N_2O emissions were 15–25% higher than for CF single rice, and 30–50% lower than for MSD single rice (Table 5). For the southern China site, N_2O emissions for the UCR scenario were the same as for the MSD double rice (Table 5). For the Thailand site, N_2O emissions were 200–300% higher than for CF single rice and 10–30% lower than for MSD single rice (Table 5). The modeled irregular pattern of N_2O fluxes related to water management is not very surprising. As an intermediate

Table 6 Baseline scenario CO_2-equivalents* ($kg\,CO_{2\text{-eq}}\,ha^{-1}\,yr^{-1}$) for CH_4 and N_2O emissions

	20 years†		100 years†		500 years†	
	CH_4	N_2O	CH_4	N_2O	CH_4	N_2O
CF single rice	9900	6800	3700	8300	1100	4100
CF double rice	8700	1700	3200	2700	970	1800
CF triple rice	18 000	6400	6600	8500	2000	5500

All values reported to two significant figures. *CF*, Continuously flooded.
*CO_2-equivalents calculated as in Eqn (3).
†Time horizon determines both mean flux (Table 4) and global warming potential (GWP) value (Table 5).

product of denitrification and nitrification, N_2O is affected by changes in the soil water regime in a very complex way. For example, more dissolved organic carbon (a by-product of decomposition that generally accumulates under submerged conditions) or lower Eh (redox potential) can stimulate denitrification, resulting either in an increase in N_2O fluxes due to more N_2O production or in a decrease in N_2O fluxes due to more N_2O being further reduced to N_2 (e.g., Davidson, 1991).

Due to methane's relatively short atmospheric lifetime/adjustment time, changes in CH_4 emissions have a larger relative impact in the near term than the long term compared with changes in N_2O emissions. Thus, for three of the six scenarios, the initial trend in the net radiative forcing was negative (i.e. cooling; Fig. 4a, b, f). However, CH_4 dominated radiative forcing over the long term in only one case (northern China CF to UCR; Fig. 4b); in this case, CH_4 emission dropped by 75% and N_2O emissions were not changed significantly (Table 4). In all other cases, N_2O dominated long-term radiative forcing, and cooling from reduced CH_4 emissions offset only 5–30% of the warming from increased N_2O emissions.

Although atmospheric burden perturbations for CO_2 were larger in absolute magnitude than for CH_4 or N_2O (Fig. 3), it played the smallest role in radiative forcing in all cases (Fig. 4). Including an upland crop in the rotation decreased the rate of soil C sequestration in all cases, because of lower yields for the upland crop than for rice, and thus, less crop residue returned to the soil. CO_2 radiative forcing was greater than 10% of the multigas net radiative forcing only for the conversion from CF rice to UCR at the northern China and Thailand sites (Fig. 4).

All results reported in the tables and figures are global atmospheric and radiative impacts per hectare of rice paddy field undergoing management change. In China, changes in water management have occurred on approximately 2×10^7 ha (Li *et al.*, 2002), and there are about 1.3×10^8 ha of rice paddy in Asia (Maclean *et al.*, 2002). Multiplying the results by 10^7–10^8, a likely range of area (hectares) that could undergo management change, gives atmospheric burden perturbations of -10 to $-300\,Tg\,CH_4$-C, 0 to $+100\,Tg\,N_2O$-N; and -0.2 to $+10\,Pg\,CO_2$-C after 500 years of changed management; current atmospheric burdens are $3650\,Tg\,CH_4$-C; $1510\,Tg\,N_2O$-N, and $730\,Pg\,CO_2$-C (Prather *et al.*, 2001; Prentice *et al.*, 2001). Scaled by 10^7–10^8, after 500 years global total radiative forcing for all three gases together ranges from -0.03 to $+0.3\,W\,m^{-2}$; note that this calculation assumes a linear relationship between atmospheric concentration and radiative forcing over 500 years, and for significant changes in gas concentrations, which is uncertain (Fuglestvedt *et al.*, 2003). Radiative forcing from changes in well-mixed greenhouse gases (CO_2, CH_4, N_2O, and halocarbons) for 1750 to present is about $+2.43\,W\,m^{-2}$ (Ramaswamy *et al.*, 2001).

Results differ across a range of sites

The three sites in this analysis were chosen to represent a gradient in climate and number of crops sown per year in the dominant rice-growing region of eastern Asia. The changes in management from CF rice paddies to midseason drainage represents a trend in paddy management in the region (e.g. Li *et al.*, 2002). By 2025, 17 million hectares of irrigated rice in Asia may experience 'physical water scarcity' and another 22 million hectares may experience 'economic water scarcity' (Cantrell, 2002). Changing agricultural management from CF to MSD with or without upland crops in the rotation has an impact on greenhouse gas emissions in all three cases, but the net impact varied from site to site. In all cases but one, changes in CH_4 or N_2O emissions had opposite effects. In one case (1-UCR), the CH_4 cooling was the dominant effect in the long term, in two cases the CH_4 impact offset more than 25% of the N_2O impact, and in three cases the CH_4 impact offset less than 13% of the N_2O impact.

In all cases over the long term (100 or 500 years), the radiative forcing due to soil carbon sequestration was smaller than the radiative forcing due to changes in either CH_4 or N_2O emissions; but its impact ranged from 1% to 28% of the net impact of CH_4 and N_2O. In two cases (2-UCR and 3-UCR) over the short term (20 years), the radiative forcing due to soil carbon sequestration was larger than net impact of CH_4 and N_2O. In some cases, the initial trend in radiative forcing was a cooling (due to reduced CH_4 emissions), but in other cases the initial trend was warming (due to increased N_2O emissions). Based on these varied results we conclude that there can be no simple prescription regarding the impact of midseason draining of rice paddies on the radiative forcing of climate. The impact is both site specific and time-horizon specific.

In the DNDC simulations, soil texture was the most significant controller of CH_4 emissions and flux differentials. SOC and its evolution in time was the most significant controller of N_2O emissions and flux differentials. Additional simulations using a wider range of values for soil texture, SOC content, and pH resulted in a greater range of results (not shown). An effective greenhouse gas emissions mitigation scenario in rice paddy agriculture cannot be as simple as a universal change to midseason draining, despite the fact that it would likely lead to reduced CH_4 emissions in virtually all situations. An effective mitigation scenario will need to take into account soil properties and additional aspects of management (especially those related to manure and crop litter inputs), current SOC content, and likely SOC trends.

Is the GWP concept adequate for realistic changes in biogeochemical cycling resulting from mitigation activities?

Changing water and crop-rotation management in paddy fields does not cause a simple pulse change in greenhouse gas emissions, nor a sustained, constant change in greenhouse gas emission. While the GWP methodology is convenient for rough comparison of gas flux impacts on radiative forcing, nearly any conceivable management strategy in a complex system like arable agriculture would result in nontrivial emissions trajectories whose impacts cannot be captured by application of the GWP methodology in a simple way. For ease of comparison, a single number like CO_2-equivalent emissions (based on a GWP value) is preferable, because then one can easily answer the overarching question: is it bigger or smaller for one scenario or another? Methodological transparency, as in a GWP calculation, is also important, so that comparisons made by any interested party produce the same results. With a varying flux, however, it does not seem that an *a priori*, simple, time-invariant analytical formulation like a GWP is possible (Wigley, 1998). And it is not clear that a single number result, like a GWP, can convey complete enough information about the impact of an emission change for fully informed decision making. Just as a mean annual global temperature contains much less information than a spatial distribution of seasonal temperatures, a single value of CO_2-equivalent emissions (e.g. based on a GWP_{100} value) contains much less information than a time series of radiative forcings. However, when comparing time series, as when comparing maps, and as opposed to when comparing single numbers, it is often difficult to reach a single, unambiguous conclusion.

Evaluation of CO_2-equivalent emissions based on the three standard GWP values (at 20-, 100-, and 500-year time horizons) gives some indication of the overall dynamic response, including the relative magnitude and sign of the overall radiative forcing (Fig. 5). In most cases where net CO_2-equivalent emissions were all negative (Fig. 5b) or all positive (Fig. 5c–e), the net radiative forcing was also always negative or positive (Table 5: 1-UCR−1-CF, 2-MSD−2-CF, 2-UCR−2-CF, and 3-MSD−3-CF). In one scenario, the 20-year time horizon CO_2-equivalent emissions were negative and the 100- and 500-year CO_2-equivalent emissions were positive (Fig. 5a; Table 5: 1-MSD−1-CF), indicating that there was an initial cooling followed by a long-term warming (Fig. 4a). In the other case (3-UCR−3-CF), CO_2-equivalent emissions were positive for 20-, 100-, and 500-year time horizons (Fig. 5f; Table 5), but the net radiative forcing was negative for the first 13 years following management change (Fig. 4f). This last case illustrates a shortcoming of using average emissions over even a relatively short period (20 years) during which emissions rates are changing rapidly, but the standard GWP methodology requires a single emission rate as an input (e.g., Eqn (5)). Calculating CO_2-equivalent emissions values for a nonconstant change in greenhouse gas flux remains problematic with the GWP methodology with fixed time horizons.

Acknowledgements

SF and CSL received support from NASA's Terrestrial Ecology Program (NAG5-12838; NAG5-7631), and, with RB, support from a NASA EOS Interdisciplinary Science project (NAG5-10135). JF received support from the European Community project METRIC (EVK2-CT-1999-00021). We thank Terje Berntsen (CICERO) for useful discussions.

References

Bouwman AF, Boumans LJM, Batjes N (2002) Modeling global annual N_2O and NO emissions from fertilized fields. *Global Biogeochemical Cycles*, **16** doi:10.1029/2001GB001812.

Brown L, Jarvis S, Sneath R *et al*. (2002) Development and application of a mechanistic model to estimate emission of nitrous oxide from UK agriculture. *Atmospheric Environment*, **36**, 917–928.

Cai Z, Sawamoto S, Li C *et al*. (2003) Field validation of the DNDC model for greenhouse gas emissions in East Asian cropping systems. *Global Biogeochemical Cycles*, **17** doi:10.1029/2003GB002046.

Cai ZC (1996) Effect of land use on organic carbon storage in soils in eastern China. *Water, Air, Soil Pollution*, **91**, 383–393.

Cai ZC, Xing GX, Shen GY *et al*. (1999) Measurements of CH_4 and N_2O emissions from rice paddies in Fengqiu, China. *Soil Science and Plant Nutrition*, **45**, 1–13.

Cantrell RP (2002) Foreword. In: *Water-wise Rice Production; Proceedings of the International Workshop on Water-wise Rice Production, 8–11 April 2002* (eds Bouman BAM, Hengsdijk H, Hardy B, Bindraban PS, Tuong TP, Ladha JK), pp. vii–viii. International Rice Research Institute, Los Baños, Philippines.

Chen GX, Huang GH, Huang B *et al*. (1995) CH_4 and N_2O emission from a rice field and effect of Azolla and fertilization on them. *Chinese Journal of Applied Ecology*, **6**, 378–382.

Davidson EA (1991) Fluxes of nitrous oxide and nitric oxide from terrestrial ecosystems. In: *Microbial Production and Consumption of Greenhouse Gases: Methane, Nitrogen Oxides, and Halomethanes* (eds Rogers J, Whitman W), pp. 219–235. American Society of Microbiology, Washington, DC.

Davidson EA, Ackerman IL (1993) Changes in soil carbon inventories following cultivation of previously untilled soils. *Biogeochemistry*, **20**, 161–193.

Frolking S, Mosier AR, Ojima DS *et al*. (1998) Comparison of N_2O emissions from soils at three temperate agricultural sites: simulations of year-round measurements by four models. *Nutrient Cycling in Agroecosystems*, **55**, 77–105.

Fuglestvedt JS, Berntsen TK, Godal O *et al*. (2003) Metrics of climate change: assessing radiative forcing and emission indices. *Climatic Change*, **58**, 267–331.

Fuglestvedt JS, Isaksen ISA, Wang W-C (1996) Estimates of indirect global warming potential for CH_4, CO and NO_x. *Climatic Change*, **34**, 404–437.

Grant B, Smith WN, Desjardins R *et al*. (2004) Estimated N_2O and CO_2 emissions as influenced by agricultural practices in Canada. *Canadian Journal of Soil Science*, in press.

Harvey LDD (1993) A guide to global warming potentials (GWPs). *Energy Pol*., **21**, 24–34.

Houghton RA (2000) Emissions of carbon from land-use change. In: *The Carbon Cycle* (eds Wigley TML, Schimel DS), pp. 63–76. Cambridge University Press, Cambridge, UK.

Huke RE, Huke EH (1997) *Rice Area by Type of Culture: South, Southeast, and East Asia*. IRRI, Los Baños, Philippines.

International Rice Research Institute (IRRI) (2002) *Riceweb*, http://www.riceweb.org/.

Johnson CE, Derwent RG (1996) Relative radiative forcing consequences of global emissions of hydrocarbons, carbon monoxide and NO_x from human activities estimated with zonally-averaged two-dimensional model. *Climatic Change*, **34**, 439–462.

Joos F, Bruno M, Fink R *et al*. (1996) An efficient and accurate representation of complex oceanic and biospheric models of anthropogenic carbon uptake. *Tellus*, **48**, 397–417.

King JY, Reeburgh WS, Thieler KK *et al*. (2002) Pulse-labeling studies of carbon cycling in Arctic ecosystems: the contribution of photosynthates to methane emission. *Global Biogeochemical Cycles*, **16**, 1062–1062.

Lashof DA, Ahuja DR (1990) Relative contributions of greenhouse gas emissions to global warming. *Nature*, **344**, 529–531.

Li C (2000) Modeling trace gas emissions from agricultural ecosystems. *Nutrient Cycling in Agroecosystems*, **58**, 259–276.

Li C, Frolking S, Butterbach-Bahl K (2004) Carbon sequestration in arable soil is likely to increase nitrous oxide emissions. *Climatic Change*, in review.

Li C, Frolking S, Frolking TA (1992) A model of nitrous oxide evolution from soil driven by rainfall events: I. model structure and sensitivity. *Journal of Geophysical Research*, **97**, 9759–9776.

Li C, Frolking S, Harriss RC (1994) Modeling carbon biogeochemistry in agricultural soils. *Global Biogeochemical Cycles*, **8**, 237–254.

Li C, Qiu JJ, Frolking S *et al*. (2002) Reduced methane emissions from large-scale changes in water management of China's rice paddies during 1980–2000. *Geophysical Research Letters*, **29** doi:10.1029/2002GL015370.

Li C, Zhuang YH, Cao MQ *et al*. (2001) Comparing process-based agro-ecosystem model to the IPCC methodology for developing a national inventory of N_2O emissions from arable lands in China. *Nutrient Cycling in Agroecosystems*, **60**, 159–175.

Li C, Zhuang YH, Frolking S *et al*. (2003) Modeling soil organic carbon change in croplands of China. *Ecological Applications*, **13**, 327–336.

Lindau CW, Patrick WH, Delaune RD *et al*. (1990) Rate of accumulation and emission of N_2, N_2O and CH_4 from a flooded rice soil. *Plant and Soil*, **129**, 269–276.

Lu YH, Watanabe A, Kimura M (2002) Contribution of plant-derived carbon to soil microbial dynamics in a paddy rice microcosm. *Biology and Fertility of Soils*, **36**, 136–142.

Maclean JL, Dawe DC, Hardy B, Hettel GP (eds) (2002) *Rice Almanac*, 3rd edn. CABI Publ., Oxon, UK.

Marland G, West TO, Schlamadinger B *et al*. (2003) Managing soil organic carbon in agriculture: the net effect on greenhouse gas emissions. *Tellus*, **55**, 613–621.

Matson PA., Naylor R., Oritz-Monasterio I. (1998) Integration of environmental, agronomic and economic aspects of fertilizer management. *Science*, **280**, 112–115.

Mosier A, Kroeze C, Nevison C *et al*. (1998) Closing the global N_2O budget: nitrous oxide emissions through the agricultural nitrogen cycle. *Nutrient Cycling in Agroecosystems*, **52**, 225–248.

Nugroho SG, Lumbanraja, Suprapto H *et al*. (1994) Effect of intermittent irrigation on methane emission from an Indonesia rice paddy field. *Soil Science and Plant Nutrition*, **40**, 609–615.

Oenema O, Velthof G, Kuikman P (2001) Technical and policy aspects of strategies to decrease greenhouse gas emissions from agriculture. *Nutrient Cycling in Agroecosystems*, **60**, 301–315.

O'Neill BC (2000) The jury is still out on global warming potentials. *Climatic Change*, **44**, 427–443.

Paustian K, Six J, Elliott ET *et al*. (2000) Management options for reducing CO_2 emissions from agricultural soils. *Biogeochemistry*, **48**, 147–163.

Prather M, Ehhalt D, Dentener F *et al*. (2001) Atmospheric chemistry and greenhouse gases. In: *Climate Change 2001: The Scientific Basis. Contribution of Working Group I to the Third Assessment Report of the Intergovernmental Panel on Climate Change* (eds Houghton JT, Ding Y, Griggs DJ *et al*.), pp. 239–287. Cambridge University Press, Cambridge, UK.

Prentice IC, Farquhar GC, Fasham MJR *et al*. (2001) The carbon cycle and atmospheric carbon dioxide. In: *Climate Change 2001: The Scientific Basis. Contribution of Working Group I to the Third Assessment Report of the Intergovernmental Panel on Climate Change* (eds Houghton JT, Ding Y, Griggs DJ *et al*.), pp. 183–237. Cambridge University Press, Cambridge, UK.

Ramaswamy V, Boucher O, Haigh J *et al*. (2001) Radiative forcing of climate change. In: *Climate Change 2001: The Scientific Basis. Contribution of Working Group I to the Third Assessment Report of the Intergovernmental Panel on Climate Change* (eds Houghton JT, Ding Y, Griggs DJ *et al*.), pp. 350–416. Cambridge University Press, Cambridge, UK.

Robertson GP, Paul EA, Harwood RR (2000) Greenhouse gases in intensive agriculture: contributions of individual gases to the radiative forcing of the atmosphere. *Science*, **289**, 1922–1925.

Sass RL, Fisher FM, Lewis ST *et al*. (1994) Methane emission from rice fields: effect of soil properties. *Global Biogeochemical Cycles*, **8**, 135–140.

Sass RL, Fisher FM, Ding A *et al*. (1999) Exchange of methane from rice fields: national, regional, and global budgets. *Journal of Geophysical Research*, **104**, 26943–26951.

Sass RL, Fisher FM, Wang YB *et al*. (1992) Methane emission from rice fields: the effect of flood water management. *Global Biogeochemical Cycles*, **6**, 249–262.

Seitzinger SP, Kroeze C (1998) Global distribution of nitrous oxide production and N inputs in freshwater and coastal marine ecosystems. *Global Biogeochemical Cycles*, **12**, 93–113.

Shine KP, Derwent RG, Wuebbles DF *et al*. (1990) Radiative forcing of climate. In: *Climate Change: The IPCC Scientific Assessment* (eds Houghton JT, Jenkins GJ, Ephraums JJ), pp. 41–68. Cambridge University Press, Cambridge, UK.

Shine KP, Fuglestvedt JS, Hailemariam K *et al*. (2004) Alternatives to the Global Warming Potential for comparing climate impacts of emissions of greenhouse gases. *Climatic Change*, in review.

Smith CJ, Brandon M, Patrick WH (1982) Nitrous oxide emission following urea-N fertilization of wetland rice. *Soil Science and Plant Nutrition*, **28**, 161–172.

Smith P, Goulding KW, Smith KA *et al*. (2001) Enhancing the carbon sink in European agricultural soils: including trace gas fluxes in estimates of carbon mitigation potential. *Nutrient Cycling in Agroecosystems*, **60**, 237–252.

Smith P, Powlson DS, Smith JU *et al*. (2000a) Meeting Europe's climate commitments: quantitative estimates of the potential for carbon mitigation by agriculture. *Global Change Biology*, **6**, 525–539.

Smith P, Smith JU, Powlson DS *et al*. (1997) A comparison of the performance of nine soil organic matter models using datasets from seven long-term experiments. *Geoderma*, **81**, 153–225.

Smith SJ, Wigley TML (2000a) Global warming potentials: 1. Climatic implications of emissions reductions. *Climatic Change*, **44**, 445–457.

Smith SJ, Wigley TML (2000b) Global warming potentials: 2. Accuracy. *Climatic Change*, **44**, 459–469.

Smith WN, Desjardins RL, Pattey E (2000b) The net flux of carbon from agricultural soils in Canada 1970–2010. *Global Change Biology*, **6**, 557–568.

Smith WN, Desjardins RL, Grant B *et al*. (2002) Testing the DNDC model using N_2O emissions at two experimental sites in Canada. *Canadian Journal of Soil Science*, **82**, 365–374.

US EPA (2002) *Inventory of U.S. Greenhouse Gas Emissions and Sinks: 1990–2000*. EPA 430-R-02-003, Office of Atmospheric Programs, U.S. Environmental Protection Agency, Washington, DC

Vörösmarty CJ, Green P, Salisbury J *et al*. (2000) Global water resources: vulnerability from climate change and population growth. *Science*, **289**, 284–288.

Wassmann R, Lantin RS, Neue HU *et al*. (2000b) Characterization of methane emissions from rice fields in Asia. III. Mitigation options and future research needs. *Nutrient Cycling in Agroecosystems*, **58**, 23–36.

Wassmann R, Neue HU, Lantin RS *et al*. (2000a) Characterization of methane emissions from rice fields in Asia: II. Differences among irrigation, rainfed, and deepwater rice. *Nutrient Cycling in Agroecosystems*, **58**, 13–22.

Watanabe A, Takeda T, Kimura M (1999) Evaluation of origins of CH_4 carbon emitted from rice paddies. *Journal of Geophysical Research*, **104**, 23623–23629.

West TO, Post WM (2002) Soil organic carbon sequestration rates by tillage and crop rotation: a global data analysis. *Soil Science Society of America Journal*, **66**, 1930–1946.

Wigley TML (1998) The Kyoto Protocol: CO_2, CH_4 and climate implications. *Geophysical Research Letters*, **25**, 2285–2288.

Yagi K, Minami K, Ogawa Y (1990) Effects of water percolation on methane emission from paddy fields. *Research Reports of the Division of Environmental Planning*, **6**, 105–112.

Yagi K, Tsuruta H, Kanda K *et al*. (1996) Effect of water management on methane emission from a Japanese rice field: automated methane monitoring. *Global Biogeochemical Cycles*, **10**, 255–267.

Zhang Y, Li C, Zhou X *et al*. (2002) A simulation model linking crop growth and soil biogeochemistry for sustainable agriculture. *Ecological Modelling*, **151**, 75–108.

Zheng XH, Wang MX, Wang YS *et al*. (1997) CH_4 and N_2O emissions from rice paddy fields in southeast China. *Scientia Atmospherica Sinica*, **21**, 231–237.